研究成果の刊行に関する一覧表

雑誌（日本語）

発表者氏名	論文タイトル名	発表誌名	巻号	ページ	出版年
林　隆一	化学放射線治療後遺残、再発症例に対する救済手術	日本気管食道科学会　会報	61（2）	111	2010
林　隆一	耳鼻咽喉科疾患の診療に関するガイドライン-解釈と有効な使い方-　頭頸部癌診療ガイドライン	JOHNS	26(5)	767-9	2010
篠﨑　剛，林　隆一	中・下咽頭におけるNBIの有用性	ENTONI	113	124-8	2010
井本 滋	センチネルリンパ節生検と腋窩リンパ節郭清	コンセンサス癌治療	9	76-7	2010
井本 滋，菅間 博，和田 徳昭	「悪性腫瘍の術中病理診断を効果的に活用するどこを検索すべきか、どう対応すべきか」乳癌	臨床外科	66	454-6	2011
井本 滋	ラジオアイソトープ（RI）法を用いた乳癌センチネルリンパ節生検手技	手術	65	409-12	2011
伊藤雅昭、齋藤典男、山本聖一郎、他	大腸癌術後フォローアップにおける経済効果の評価	大腸疾患NOW		187-95	2010
伊藤雅昭、齋藤典男.	腹腔鏡家内肛門括約筋切除術（腹腔鏡下ISR）、	Digestive Surgery NOW、下部消化管の腹腔鏡下手術	No.9	88-106	2010
伊藤雅昭、齋藤典男.	直腸癌手術における肛門温存(7)下部直腸癌に対する肛門温存手術後の機能評価、	臨牀消化器内科	25(1)	63-72	2010
伊藤雅昭、角田祥之、甲田貴丸、齋藤典男.	大腸癌におけるPET/CT検査の意義、	臨床外科	65(2)	224-30	2010
中嶋健太郎、小林昭広、甲田貴丸、齋藤典男他	痔瘻癌15例の臨床病理学的検討、	日本大腸肛門病学会雑誌	63	346-58	2010
伊藤雅昭、齋藤典男	〈特集〉消化管再建法－合併症ゼロへの工夫－Ⅲ.腸切除後の再建法、6.ISRにおける再建法	手術	64(10)	1517-23	2010

研究成果の刊行に関する一覧表

西澤雄介、伊藤雅昭、小林昭広、杉藤正典、齋藤典男、	腹腔鏡下手術　横行結腸切除術、	臨床外科	65(11)	312-18	2010
西澤祐吏、伊藤雅昭、甲田貴丸、齋藤典男、他	腹腔鏡下直腸癌手術における前壁剥離の工夫、	臨床外科	65(12)	1581-5	2010
佐々木寛.	婦人科がん術後下肢リンパ浮腫を予防する鍵は後腹膜開放と大腿ソケイ上リンパ節温存.	日本リンパ学会機関誌	30 (2)	131-2	2010
飯田泰志、佐々木寛.	リンパ浮腫に関する新たな検討と試み.	産科と婦人科	77(9)	1083-88	2010
佐々木寛、飯田泰志.	下肢リンパ浮腫予防手術. 59(8):1123-28. 2010	産婦人科の実際	59(8)	1123-28	2010
山田恭輔、岡本愛光、矢内原臨、佐々木寛、他	卵巣癌治療における新たな展開再発卵巣癌に対する腫瘍減量手術.	日本婦人科腫瘍学会雑誌	28 (3)	396-402	2010
井本 滋, 菅間 博, 和田徳昭	「悪性腫瘍の術中病理診断を効果的に活用する -どこを検索すべきか、どう対応すべきか-」乳癌	臨床外科	66	454-6	2011
井本 滋	ラジオアイソトープ（RI）法を用いた乳癌センチネルリンパ節生検手技	手術	65	409-12	2011
井本 滋	術前化学療法とセンチネルリンパ節生検	臨床外科	66	882-5	2011
井本 滋	「進歩する癌転移診断 - 外科臨床はどう変わるのか」乳癌	臨床外科	66	1312-6	2011
伊東 大樹, 井本 滋	治療検査（治療モニタリングと腫瘍マーカー）	治療	93	1242-5	2011
井本 滋	センチネルリンパ節生検について	治療	93	1074-6	2011

研究成果の刊行に関する一覧表

齋藤典男、杉藤正典、伊藤雅昭、小林昭広、西澤雄介	下部直腸癌に対する周術期（術前・術後）化学放射線療法の有用性、大腸癌－最新の研究の動向－、Ⅷ.大腸癌の治療戦略放射線療法	日本臨床	69(3)	500-4	2011
西澤祐吏、藤井誠志、齋藤典男、伊藤雅昭、杉藤正典、小林昭広、西澤雄介、中嶋健太郎、甲田貴丸、錦織英知	ISR術前化学放射線療法における術後肛門機能に関する組織学的要因	癌の臨床	56(8)	575-8	2011
甲田貴丸、伊藤雅昭、齋藤典男、杉藤正典、小林昭広、西澤雄介、西澤祐吏、中嶋健太郎	術前放射線化学療法のISR術後肛門機能へ与える影響	癌の臨床	56(8)	579-84	2011
齋藤典男、杉藤正典、伊藤雅昭、小林昭広、西澤雄介	直腸癌に対する低位前方切除術	手術	65(6)	905-12	2011
齋藤典男、伊藤雅昭、小林昭広、西澤雄介、杉藤正典	直腸癌に対する肛門温存手術	日外会誌	112(5)	318-24	2011
佐々木寛、佐々木徹、多田春江、飯田泰志、武石明精	婦人科癌術後の下肢リンパ浮腫の危険要因と後腹膜大腿ソケイ部でのリンパ管静脈吻合術の有効性	日本マイクロサージャリー学会会誌	24-3	240-7	2011
高野浩邦，河西十九三，早田篤子，立花美津子，石塚康夫，茂木真，小竹譲，生水真紀夫，佐々木寛，田中忠夫	子宮頸がん検診へのベセスダシステム2001導入による不適正検体の頻度の実際とその推移	日本臨床細胞学会雑誌	50-3	158-62	2011
池田公史	ソラフェニブの副作用対策（手足症候群・下痢・高血圧など）	医学のあゆみ	236	711-5	2011
池田公史	臨床で分子標的薬を使用する際のポイント　肝細胞癌	Prog. Med.	31	2607-13	2011
森田達也，野末よし子，花田芙蓉子，宮下光令，鈴木聡，木下寛也，白髭豊，江口研二	地域対象の緩和ケアプログラムによる医療福祉従事者の自覚する変化：OPTIM-study.	Palliat Care Res	7巻1号	121-35	2012
林　隆一	高齢者に対する外科治療 ―頭頸部―	日気食会報	65(5)	362-397	2012

研究成果の刊行に関する一覧表

井本 滋	乳癌センチネルリンパ節生検	外科	74	699-703	2012
井本 滋	センチネルリンパ節転移陽性乳癌における腋窩治療	腫瘍内科	10	122-125	2012
井本 滋	乳癌治療の現状と展望	杏林医学会雑誌	43	145-150	2013
伊藤雅昭、齋藤典男、杉藤正典、小林昭広、西澤雄介、	腹腔鏡下大腸切除術 腹腔鏡下ISR	消化器外科	35(1)	67-79	2012
小林昭広、伊藤雅昭、西澤雄介、小林昭広、杉藤正典、齋藤典男、	腹腔鏡下大腸癌手術に伴う偶発症の検討	日本腹部救急医学会雑誌	32(1)	37-42	2012
神山篤史、齋藤典男、杉藤正典、伊藤雅昭、小林昭広、西澤雄介、	進行直腸癌における肛門温存手術	手術	66(2)	179-184	2012
伊藤雅昭、齋藤典男、杉藤正典、小林昭広、西澤雄介、	腹腔鏡下ISR	手術	66(6)	901-908	2012
菅野伸洋、伊藤雅昭、中嶋健太郎、櫻庭　実、杉藤正典、小林昭広、西澤雄介、錦織英知、神山篤史、齋藤典男	超低位前方切除あるいはISR術後の吻合部狭窄	消化器外科	35(11)	1647-1654	2012
野口幸子、佐薙佳世、武隈桂子、髙橋一彰、森本恵爾、小曽根浩一、田部宏、小竹譲、髙野浩邦、佐々木寛　他	巨大卵巣腫瘍に対して当院で施行している小切開No Leak法の検討	千葉産科婦人科学会雑誌	6：1	10-14	2012
池田公史、光永修一、清水怜、大野泉、高橋秀明、奥山浩之、桑原明子、奥坂拓志	進行肝細胞癌に対するソラフェニブの現状と今後の展望	日本消化器病学会雑誌	109(8)	1346-54	2012
全田貞幹	頭頸部扁平上皮癌に対する新しい治療戦略　放射線治療の新しいモダリティー	JOHNS	28(8)	1185-1189	2012
森田達也、木下寛也、他	地域緩和ケアプログラムに参加した医療福祉従事者が地域連携のために同職種・他職種に勧めること	Palliat Care Res	7(1)	163-171	2012

研究成果の刊行に関する一覧表

木下寛也、森田達也、他	がん専門病院が地域緩和ケアの向上のために取り組んでいることと課題	癌と化学療法	39(10)	1527-1532	2012
木澤義之、木下寛也、森田達也、他	地域で統一した緩和ケアマニュアル・パンフレット・評価シートの評価：OPTIM-study	Palliat Care Res	7(2)	172-184	2012
森田達也、木下寛也、他	地域緩和ケアプログラムに参加した医療福祉従事者が最も大きいと体験すること：OPTIM-study	Palliat Care Res	7(2)	209-217	2012
木下寛也、森田達也、他	がん専門病院緩和ケア病棟の運営方針が地域の自宅がん死亡率に及ぼす影響	Palliat Care Res	7(2)	348-353	2012
森田達也、木下寛也、他	異なる算出方法による地域での専門緩和ケアサービス利用数の比較	Palliat Care Res	7(2)	374-381	2012
森田達也、木下寛也、他	患者所持型情報共有ツール「わたしのカルテ」の評価：OPTIM-study	Palliat Care Res	7(2)	382-388	2012
東陽一郎、木下寛也	新しい局面を迎えた肺癌診療《肺癌診療にまつわるトータルサポート　治療とケア》緩和ケアの実際	内科	110(5)	771-774	2012
井本 滋	ラジオ波焼灼治療の現状	臨床と研究	90 (10)	1311-1315	2013
齋藤典男、酒井泰之、駒井好信、伊藤雅昭、小林昭広、西澤雄介、杉藤正典、	局所高度進行直腸癌に対する外科治療　a)隣接臓器合併症を伴う拡大切除	外科	75(3)	250-256	2013
山崎信義、杉藤正典、神山篤史、西澤雄介、小林昭広、伊藤雅昭、斎藤典男、	回腸導管作成術後に空腸導管症候群様症状を来した1例	日本大腸肛門病学会誌	66	353-357	2013
齋藤典男、伊藤雅昭、小林昭広、西澤雄介、杉藤正典、横田　満、佐藤　雄	長期観察からみたI SRの意義	癌の臨床	59	673-679	2013

研究成果の刊行に関する一覧表

赤木由人、伊藤雅昭、齋藤典男、白水和雄、前田耕太郎、金光幸秀、幸田圭史、長谷和生、山中竹春、森谷宜皓、	肛門近傍の下部直腸癌に対する肛門括約筋部分温存術の多施設共同第Ⅱ相試験	癌の臨床	59	643-649	2013
河野眞吾、齋藤典男、合志健一、塚田祐一郎、山崎信義、西澤雄介、小林昭広、伊藤雅昭、	長期成績を左右する手術手技のポイント－腹腔鏡手術によるISR	臨床外科	69(3)	314-317	2013
佐々木寛	婦人科がん術後下肢リンパ浮腫の予防手術	がんのリハビリテーションセミナー新・リンパ浮腫研修			in press
髙野浩邦, 佐々木寛.	【プロメテウス　婦人科がん最新医療】ロボット支援手術	産婦人科の実際	62巻12号	2071-2076	2013
佐々木寛.	液状化検体細胞診加算	検査と技術	41巻12号	1187-1189	2013
小曽根浩一, 佐々木寛.	【細胞診の基礎から実践へ】細胞診断の基本　検診の現状（婦人科、呼吸器）	病理と臨床	31巻臨増	87-92	2013
全田貞幹 秋元哲夫	鼻・副鼻腔悪性腫瘍に対する陽子線治療	頭頸部癌	39(4)	402-4	2013
全田貞幹	局所進行頭頸部扁平上皮癌に対する国内第Ⅱ相試験	頭頸部癌FRONTIER	1(2)	30-2	2013
全田貞幹	放射線治療による有害事象軽減のための支持療法	JOHNS	29(6)	1051-4	2013
飯野京子，綿貫成明，小山友里江，栗原美穂，市川智里，岡田教子，上杉英生, 淺沼智恵, 大幸宏幸, 藤田武郎, 鈴木恭子，和田千穂子，森美知子, 久部洋子，矢ヶ崎香，小松浩子	胸部食道がん術後外来患者に対する看護ケアの分析.	Palliat Care Research			2014 in press
綿貫成明, 飯野京子, 小山友里江，栗原美穂，市川智里，岡田教子，上杉英生, 淺沼智恵, 大幸宏幸, 藤田武郎, 鈴木恭子，和田千穂子，森美知子, 久部洋子，矢ヶ崎香，小松浩子.	胸部食道がん術後患者の退院後の生活における困難の実態	Palliat Care Research	9 (1)	129－136	2014 in press

厚生労働科学研究費補助金

第3次対がん総合戦略研究事業

「QOLの向上をめざしたがん治療法の開発研究」

に関する研究

平成22年度～平成25年度　総合研究報告書

研究代表者　　江角　浩安

平成26（2014）年　5月

平成22年度

研究成果の刊行物・別刷

Cancer Science
The official journal of the Japanese Cancer Association JCA

Hypoglycemic/hypoxic condition *in vitro* mimicking the tumor microenvironment markedly reduced the efficacy of anticancer drugs

Hiroko Onozuka,[1,2] Katsuya Tsuchihara[1] and Hiroyasu Esumi[1,2,3]

[1]Cancer Physiology Project, Research Center for Innovative Oncology, National Cancer Center Hospital East, Kashiwa, Chiba; [2]Department of Integrated Biosciences, Graduate School of Frontier Sciences, The University of Tokyo, Kashiwa, Chiba, Japan

(Received November 23, 2010/Revised January 14, 2011/Accepted January 18, 2011/Accepted manuscript online January 21, 2011/Article first published online March 7, 2011)

Tumor tissues are often hypoxic because of defective vasculature. We previously showed that tumor tissues are also often deprived of glucose. The efficacy of anticancer drugs is affected by the tumor microenvironment, partly because of the drug delivery and cellular drug resistance; however, the precise mechanisms remain to be clarified. In the present study, we attempted to clarify whether hypoglycemic/hypoxic condition, which mimics the tumor microenvironment, might induce drug resistance, and if it did, to elucidate the underlying mechanisms. Pancreatic cancer-derived PANC-1 cells were treated with serial dilutions of anticancer drugs and incubated in either normoglycemic (1.0 g/L glucose) or hypoglycemic (0 g/L glucose) and normoxic (21% O_2) or hypoxic (1% O_2) conditions. The 50% inhibitory concentration of gemcitabine was 1000 times higher for PANC-1 cells incubated under the hypoglycemic/hypoxic condition than for those incubated under the normoglycemic/normoxic condition. Conventional anticancer drugs target rapidly growing cells, so that non-proliferating or slowly proliferating cells usually show resistance to drugs. Though the cell cycle was delayed, sufficient cellular uptake and DNA incorporation of gemcitabine occurred under the hypoglycemic/hypoxic condition to cause DNA lesions and S-phase arrest. To overcome hypoglycemic/hypoxia-induced drug resistance, we examined kinase inhibitors targeting Chk1 or cell-survival signaling pathways. Among the compounds examined, the combination of UCN-01 and LY294002 partially sensitized the cells to gemcitabine under the hypoglycemic/hypoxic condition. These findings suggested that the adoption of suitable strategies may enhance the cytotoxicities of clinically used anticancer drugs against cancer cells. (*Cancer Sci* 2011; 102: 975–982)

It is widely accepted that solid tumors are heterogeneous in structure as a result of unregulated cancer cell proliferation, presence of several cell types and aberrant vessel formation. Among these, the tumor vasculature has a major impact on the tumor microenvironment. In normal tissue, vascular networks generally develop in a well-ordered hierarchal fashion, so that an insufficient blood supply seldom occurs. In contrast, tumor vascular networks undergo continuous remodeling, because unregulated cell proliferation destroys the existing tissue structures. Previous structural analyses had clearly shown that tumors exhibit aberrant and poorly organized vasculature without any hierarchy.[1–4]

As a consequence of the poorly organized vasculature in tumors, the delivery of oxygen is extremely limited. Direct measurement of the oxygen tension in cancer tissues has demonstrated the presence of severely hypoxic regions in many types of cancers.[5] Although hypoxia is also toxic to cancer cells, cancer cells adapt through genetic and epigenetic changes that allow them to survive and even proliferate in hypoxic environments.[6–9] Hypoxia-inducible factor-1α (HIF-1α) is a key transcription factor for downstream hypoxia-inducible genes, which regulate several biological processes in hypoxic environments.[10–12] Hypoxia response pathways overlap with many of the known oncogenic signaling pathways and also contribute to tumor aggressiveness.[13–15] Therefore, tumor hypoxia is regarded as a good target for cancer therapy. Meanwhile, cancer cells predominantly use the glycolytic pathway, rather than oxidative phosphorylation, for energy production, irrespective of the oxygen availability (Warburg effect).[16,17] In addition to the intrinsic predisposition of cancer cells to metabolize glucose, HIF-1α has been shown to regulate the expressions of all the enzymes involved in the glycolytic pathway, which mediate cellular glucose uptake.[18,19] The activation of HIF-1α enables cancer cells to use excessive glucose to maintain cellular homeostasis in hypoxic environments, causing depletion of glucose from the surrounding tissues. Indeed, a metabolomic analysis of stomach and colon cancer tissues has clearly showed glucose depletion in the tumor tissues as compared to normal tissues, indicating that several regions of tumor tissues are characterized by both hypoxia and hypoglycemia.[20] However, little is known about the biology of cancer cells under hypoglycemic condition.

Although many molecular-targeting drugs have been introduced for clinical use, conventional anticancer drugs are in wide clinical use and continue to confer many clinical benefits. Heterogeneity in the tumor microenvironment provides cancer cells the opportunity to escape from anticancer drugs. One of the processes affected by the heterogeneity of tumors is drug diffusion.[21,22] In addition, many types of drug resistance of the cells to anticancer drugs are known to occur, and overexpression of the ABC transporter is a representative mechanism.[23–25] Recent studies have reported that drug resistance may also be related to the tumor microenvironment, especially hypoxia, and the clinical relevance of such resistance. Three-dimensional culture system is used as a useful new strategy to represent tumor microenvironment *in vitro*.[26,27] However, the detailed molecular mechanisms for the resistance are largely unclear. In this study, we clarified how hypoglycemic/hypoxic condition might affect the efficacies of anticancer drugs.

Materials and Methods

Cell lines and culture conditions. The human pancreatic ductal adenocarcinoma cell lines PANC-1 and Capan-1 and the hepatoma-derived cell line HepG2 were purchased from ATCC (American Type Culture Collection, Rockville, MD, USA). PSN-1 was gifted from the Genetics Division of the National Cancer Center Research Institute (Tokyo, Japan). All cell lines were maintained in DMEM (Nissui, Tokyo, Japan). A

[3]To whom correspondence should be addressed. E-mail: hesumi@east.ncc.go.jp

doi: 10.1111/j.1349-7006.2011.01880.x

glucose-deprived condition was achieved by culturing the cells in glucose-free medium (Sigma, St. Louis, MO, USA). A hypoxic condition was achieved by incubating the cells in a hypoxia incubator in the presence 5% CO_2 and 1% O_2. The experiments were performed using PANC-1 cells, unless stated otherwise.

Reagents. Gemcitabine (Gemzar; Eli Lilly Co., Indianapolis, IN, USA) and 5-fluorouracil (Kyowa Hakko Kirin Co., Ltd, Tokyo, Japan) were dissolved in saline and stored at −20°C. Cisplatin (Sigma) was dissolved in DMSO on the day of use. UCN-01 was kindly provided by Kyowa Hakko Kirin Co., Ltd. LY294002 and Gö6976 were purchased from Calbiochem (San Diego, CA, USA). Antibodies were purchased from the following manufacturers: anti-total Akt, anti-phosphospecific Akt (Ser 473), anti-phosphospecific Cdc25c (Ser216), anti-phosphor specific Chk1 (Ser345), anti-phosphospecific Chk2 (Thr68), and anti-γ-H2AX (Ser139) from Cell Signaling Technology (Danvers, MA, USA); anti-HIF-1α and anti-HIF-2α antibodies from Novus Biologicals (Littleton, CO, USA); Chk1 (G-4) and Actin (C-11) antibodies from Santa Cruz Biotechnology (Santa Cruz, CA, USA); Chk2 antibody clone7 from Upstate Biotechnology (Lake Placid, NY, USA). The following secondary antibodies were purchased from Santa Cruz Biotechnology: goat antimouse IgG-HRP, goat antirabbit IgG-HRP, and donkey antigoat IgG-HRP.

Cytotoxicity assay of anticancer drugs. The cytotoxicity assay was performed using Cell Counting kit-8 (Dojindo Molecular Technologies, Kumamoto, Japan), as described previously.[28] The cell number in the absence of anticancer drugs under each culture condition was set as 100%. Values shown represent the means ± SD (n = 4–8).

siRNA transfection. SMARTpool HIF-1α, HIF-2α, Chk1, Chk2 and non-silencing siRNA were purchased from Dharmacon (Lafayette, CO, USA). Cells were seeded at 10^6 cells per dish in 10 mm dishes. At 24 h after seeding, siRNA was added at a final concentration of 100 nM, followed by incubation for 24 h. The knockdown efficacies were determined by Western blot analysis.

Western blot analysis. Protein extraction and Western blot analysis were performed as described previously.[29] The antibody dilutions used were in accordance with the manufacturers' instructions.

Cell cycle analysis. After 24 h preincubation, 1×10^6 cells were cultured in a 60-mm cell culture dish under either normoglycemic/normoxic or hypoglycemic/hypoxic conditions for 24 h, followed by staining using the Click-iT EdU Alexa Fluor 488 Cell Proliferation Assay kit (Molecular Probes, Eugene, OR, USA) in accordance with the manufacturer's instructions, and analyzed on a FACSCalibur (BD Bioscience, San Jose, CA, USA).

DNA ploidy assay. After 24 h preincubation, 1×10^6 cells were cultured in a 60-mm cell culture dish under either normoglycemic/normoxic or hypoglycemic/hypoxic conditions in the presence or absence of 1 μM gemcitabine for 24 h, followed by staining with propidium iodide (Molecular Probes) in accordance with the manufacturer's instruction, and analyzed on a FACSCalibur.

[^{3}H]-Gemcitabine and [^{3}H]-thymidine uptake. After 24 h preincubation, 1×10^6 cells were cultured in a 60-mm cell culture dish under either normoglycemic/normoxic or hypoglycemic/hypoxic conditions for 24 h, followed by incubation for another 3 h with 1 μM [^{3}H]-labeled gemcitabine (6.8 μCi/nmol; Moravek Biochemicals, Brea, CA, USA). The cells were washed thrice with complete medium containing 100 μM gemcitabine, and twice with ice-cold PBS. The cells were detached by trypsinization and counted by the Trypan blue exclusion method. The total cellular uptake of [^{3}H]-gemcitabine was measured by lysing a 10 μL aliquot of the cell suspension and counting the total cell-associated radioactivity using a multipurpose scintillation counter, LS6500 (Beckman Coulter Inc., Fullerton, CA, USA). The incorporation of [^{3}H]-gemcitabine into the DNA was determined by a previously published method, with slight modification.[30]

Statistical analysis. All the results were expressed as the mean ± SD. The statistical analysis was conducted using the Student t-test after an ANOVA.

Results

Effect of the culture condition on the sensitivity to various anticancer drugs. In the first set of experiments, we determined whether hypoxia and hypoglycemia might affect the sensitivity of the cancer cells to gemcitabine, 5-fluorouracil and cisplatin, which are commonly used drugs for systemic chemotherapy of cancer. Pancreatic cancer-derived PANC-1 cells were treated with serial dilutions of anticancer drugs and incubated under either a normoglycemic (1.0 g/L glucose) or hypoglycemic (0 g/L glucose) condition and normoxic (21% O_2) or hypoxic (1% O_2) condition. The 50% inhibitory concentration (IC_{50}) of gemcitabine for the PANC-1 cells incubated under the normoglycemic/normoxic condition was 300 nM, whereas the IC_{50} values of gemcitabine under the hypoxic and hypoglycemic condition were >300 μM, which was 1000 times higher than the value under the normoglycemic/normoxic condition (Fig. 1A). Similarly, the IC_{50} of 5-fluorouracil was greatly influenced by the culture condition, with IC_{50} values of 2.7 μM under the normoglycemic/normoxic condition, 9.6 μM under the hypoglycemic/normoxic condition, 92 μM under the normoglycemic/hypoxic condition, and 79 μM under the hypoglycemic/hypoxic condition (Fig. 1B); the corresponding values for cisplatin were 74, 106, 108 μM, and more than 300 μM (Fig. 1C). The cytotoxicities of gemcitabine for other pancreatic cancer cell lines, PSN-1 and Capan-1, were also examined. The IC_{50} of gemcitabine for the PSN-1 cells was 0.22 μM under the normoglycemic/normoxic condition and more than 300 μM under the hypoglycemic/hypoxic condition (Fig. 1D). The IC_{50} of gemcitabine for the Capan-1 cells was 0.24 μM under the normoglycemic/normoxic condition, and 57 μM under the hypoglycemic/hypoxic condition (Fig. 1E). The sensitivities of the hepatoma-derived HepG2 cells, which express wild-type p53, were also examined. The IC_{50} of gemcitabine for HepG2 cells was 2.9 μM under the normoglycemic/normoxic condition, and more than 300 μM under the hypoglycemic/hypoxic condition (Fig. 1F).

Cell-cycle progression and gemcitabine uptake under various culture conditions. During cell proliferation, cells must prepare to double all their components. The restriction of nutrient and oxygen supply might greatly influence the cell-cycle progression, through complex mechanisms.[31] Gemcitabine is incorporated into the DNA to exert its cytotoxicity.[32,33] Therefore, the cell-cycle analysis was conducted under the hypoglycemic/hypoxic condition. Newly synthesized DNA was labeled with 5-ethynil-2′-deoxyuridine (EdU), and the DNA content was labeled with 7-aminoactinomycin D, followed by multicolor analysis by flow-cytometry. About 45% of the cells under the normoglycemic/normoxic condition and 41% of the cells under the hypoglycemic/hypoxic condition were in the S-phase. Thus, the S-phase population was almost the same under both conditions. Closer analysis of the S-phase populations under both conditions indicated that the numbers of cells in the late S and G2 phases were reduced under the hypoglycemic/hypoxic condition, indicating S-phase prolongation (Fig. 2A). The cellular uptake and DNA incorporation of gemcitabine were directly assessed using [^{3}H]-labeled gemcitabine. Cells were cultured under the normoglycemic/normoxic or hypoglycemic/hypoxic condition for 24 h, followed by incubation with 1 μM [^{3}H]-gemcitabine for 3 h. The cellular uptake of gemcitabine was almost

doi: 10.1111/j.1349-7006.2011.01880.x

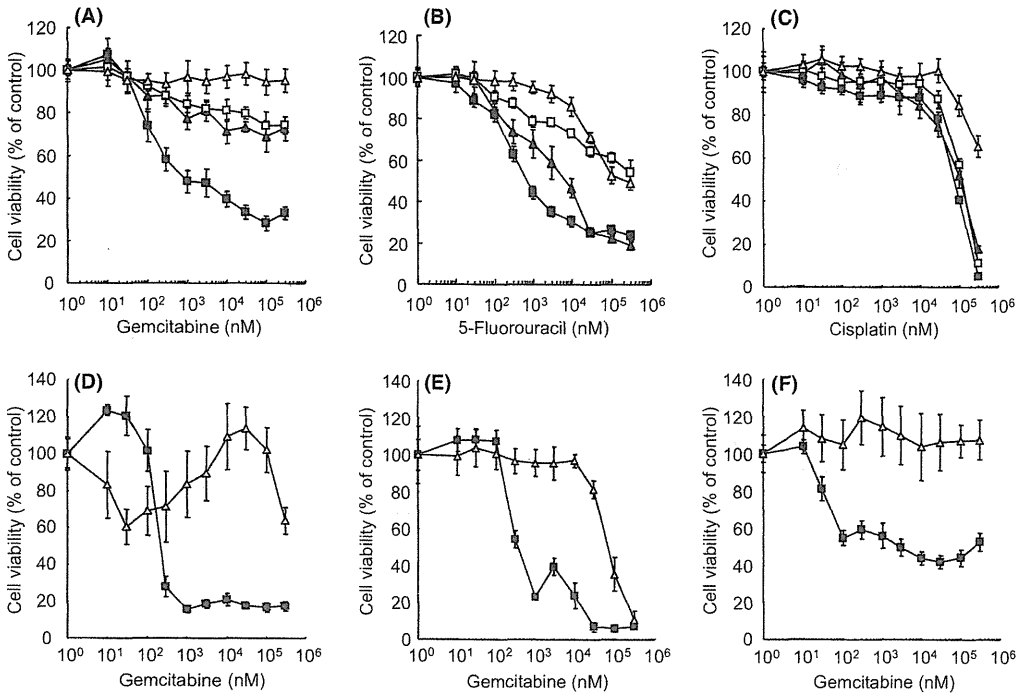

Fig. 1. Effect of the culture condition on the cytotoxicity of anticancer drugs. The cytotoxicity of (A) gemcitabine, (B) 5-fluorouracil and (C) cisplatin on the PANC-1 cells was examined. Cytotoxicity of gemcitabine on (D) the Capan-1, (E) PSN-1 and (F) HepG2 cells were also examined. (■) normoglycemic/normoxic, (▲) hypoglycemic/normoxic, (□) normoglycemic/hypoxic, and (△) hypoglycemic/hypoxic conditions.

twofold higher and the DNA incorporation of [^{3}H]-gemcitabine was almost fivefold higher under the hypoglycemic/hypoxic condition than under the normoglycemic/normoxic condition (Fig. 2B).

Gemcitabine-induced checkpoint activation and S-phase arrest. DNA incorporation of gemcitabine cause the replication fork to stall; this, in turn, induces S-phase checkpoint activation and S-phase arrest or apoptosis.[34,35] To analyze the signaling by gemcitabine-induced DNA lesions, we examined checkpoint kinase activations. After 12 h incubation in the presence or absence of 1 and 100 μM gemcitabine, phosphorylation of H2AX, Chk1 and Chk2 were induced by gemcitabine equally under different culture conditions (Fig. 2C). We further examined gemcitabine-induced S-phase arrest using propidium iodide staining and flow-cytometric analysis. S-phase arrest was equally induced by gemcitabine under the normoglycemic/normoxic and hypoglycemic/hypoxic conditions (Fig. 2D).

Effect of inhibition of Chk1 signaling on the cytotoxicity of gemcitabine. Previous studies have shown that UCN-01 and Gö6976 sensitized cells to gemcitabine via Chk1 inhibition, resulting in abrogation of the cell cycle arrest and subsequent cell death.[36–39] We examined the sensitivity of Chk1 signaling-inhibited cells to gemcitabine under the hypoglycemic/hypoxic condition. Western blot analysis showed that 1 μM of the Chk1 inhibitors, UCN-01 and Gö6976, reduced the phosphorylation of cdc25c, a downstream mediator of Chk1 (Fig. 3A); UCN-01 and Gö6976 lowered the IC_{50} of gemcitabine by more than 10 times under the normoglycemic/normoxic condition, but not under the hypoglycemic/hypoxic condition (Fig. 3B,C). Similar results were obtained with 10 μM UCN-01 or Gö6976. To confirm these results, the effect of an RNAi for Chk1 was examined. The RNAi effectively suppressed Chk1 activation under both the normoglycemic/normoxic and hypoglycemic/hypoxic conditions (Fig. 3D); however, Chk1 suppression enhanced the sensitivity of the cells to gemcitabine only under the normoglycemic/normoxic condition (Fig. 3E).

Effect of inhibition of the HIFs and PI3K/Akt signaling on the sensitivity of the cancer cells to gemcitabine. HIF-1α is induced by hypoxia and modifies cell survival.[40,41] Under the hypoxic condition, the HIF-1α protein levels increased rapidly to peak within 2 h and thereafter decreased (Fig. 4A). The HIF-2α protein level was also rapidly induced within 2 h, and maintained for 24 h. The HIF-1α protein level decreased, but not the HIF-2α protein levels, under the hypoglycemic condition (Fig. 4A). To evaluate the involvement of the HIFs in the resistance to gemcitabine, HIF-1α or HIF-2α expression was suppressed by RNAi and the sensitivity of the cells to gemcitabine was examined. RNAi for HIF-1α and HIF-2α effectively suppressed the hypoxia-induced accumulation of the respective proteins (Fig. 4B). Knockdown of HIF-1α, HIF-2α or HIF-1/2α did not have any effect on the sensitivity of the cells to gemcitabine under hypoxic condition (Fig. 4C–E). Akt is known to be activated by hypoglycemic condition and to play some roles in cell survival.[42,43] In our study, marked increase of Akt phosphorylation at ser473 was observed within 2 h under both the hypoglycemic and hypoxic condition, which was sustained for at least 24 h; the increase was, however, more evident under the hypoxic condition (Fig. 4A). To examine the involvement of PI3K/Akt signaling in the drug resistance, we utilized a PI3K inhibitor, LY294002. After treatment with LY294002 (10 and 20 μM) for 24 h, Akt phosphorylation was effectively inhibited to less than the basal level (Fig. 4F). Although treatment with 20 μM of LY294002 reduced the IC_{50} of gemcitabine by 15-fold under the normoglycemic/normoxic condition, it had little effect under the hypoglycemic/normoxic condition (Fig. 4G).

Effect of combined inhibition of Chk1 and HIF signaling on the drug resistance induced by hypoglycemic/hypoxic condition. Inhibition of either checkpoint to produce release from the gemcitabine-induced S-phase arrest or of cell-survival signaling under hypoxia, HIFs, and under hypoglycemia Akt, each alone was not effective to ameliorate the resistance to gemcitabine. We examined the combined inhibition of Chk1 and

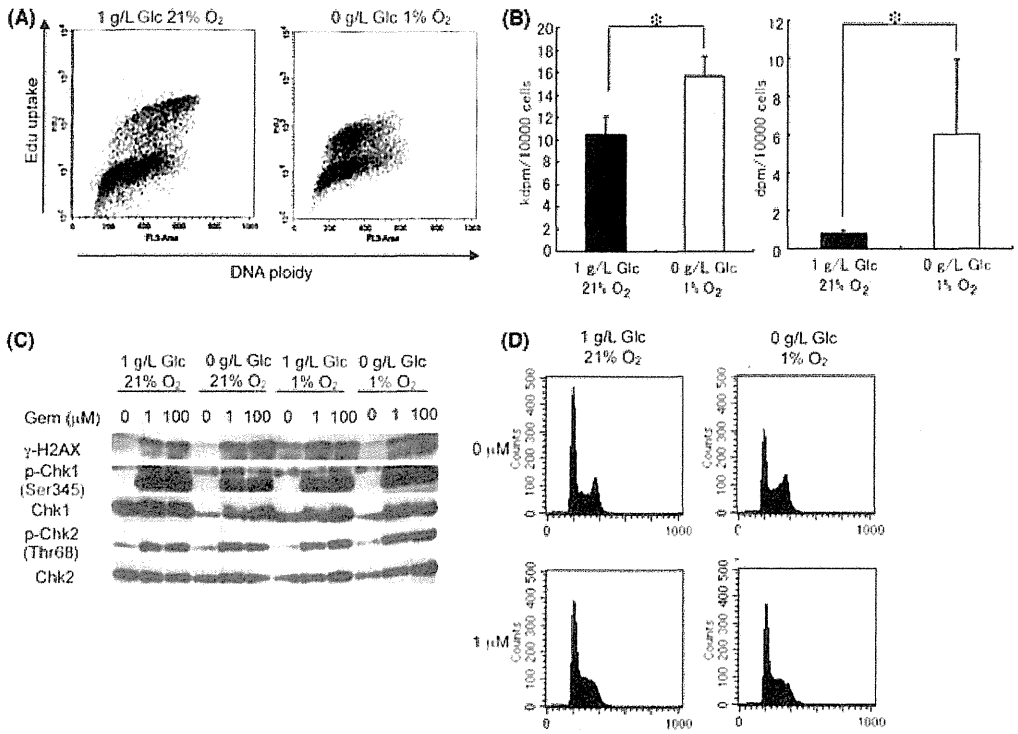

Fig. 2. Cell-cycle progression, uptake of gemcitabine and gemcitabine-induced cellular responses under various conditions. (A) Representative cell-cycle distribution detected by EdU incorporation and flow cytometry. Three independent experiments were carried out. (B) Cellular uptake and DNA incorporation of [^{3}H] gemcitabine (*$P < 0.05$). (C) Phosphorylations of H2AX, Chk1 and Chk2 detected by Western blot analysis after 12 h treatment with the indicated concentration of gemcitabine. (D) Representative DNA ploidy patterns after 24 h treatment with 1 μM gemcitabine. Three independent experiments were carried out.

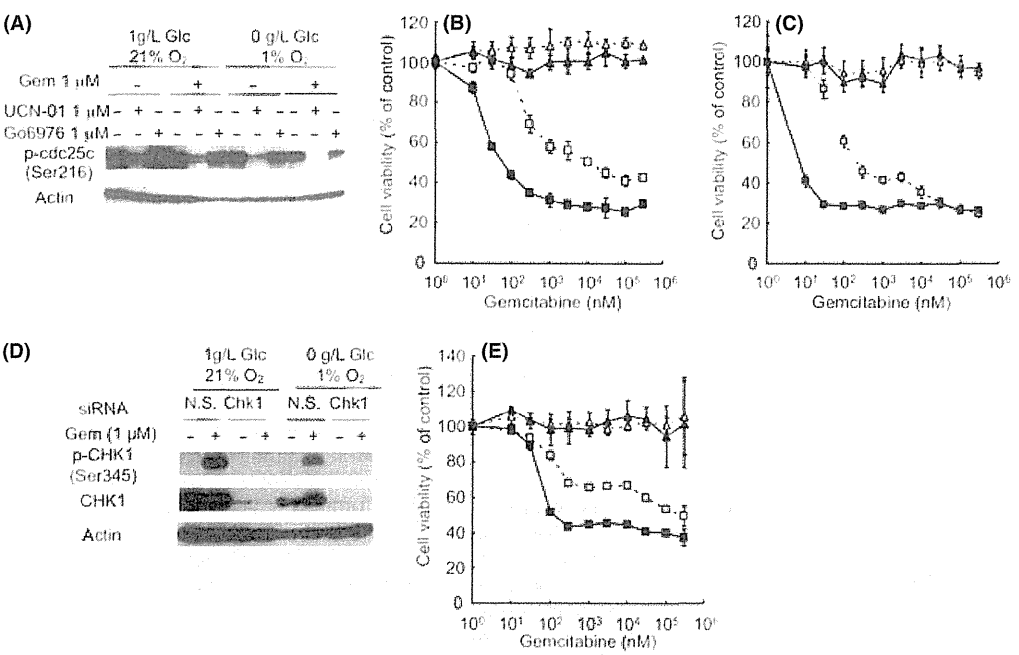

Fig. 3. Effect of inhibition of Chk1 signaling on the sensitivity of cells to gemcitabine. (A) Western blot analysis of cdc25c in the presence of Chk1 inhibitors under the indicated conditions. Cytotoxicity of gemcitabine in the presence or absence of 1 μM (B) UCN-01, (C) or Gö6976 under (■ or □) normoglycemic/normoxic condition or (▲ or △) hypoglycemic/normoxic condition. (D) Western blot analysis of Chk1 expression and activation. (E) The cytotoxicity of gemcitabine with or without Chk1 knockdown under (□ or ■) normoglycemic/normoxic condition or (△ or ▲) hypoglycemic/hypoxic condition.

doi: 10.1111/j.1349-7006.2011.01880.x

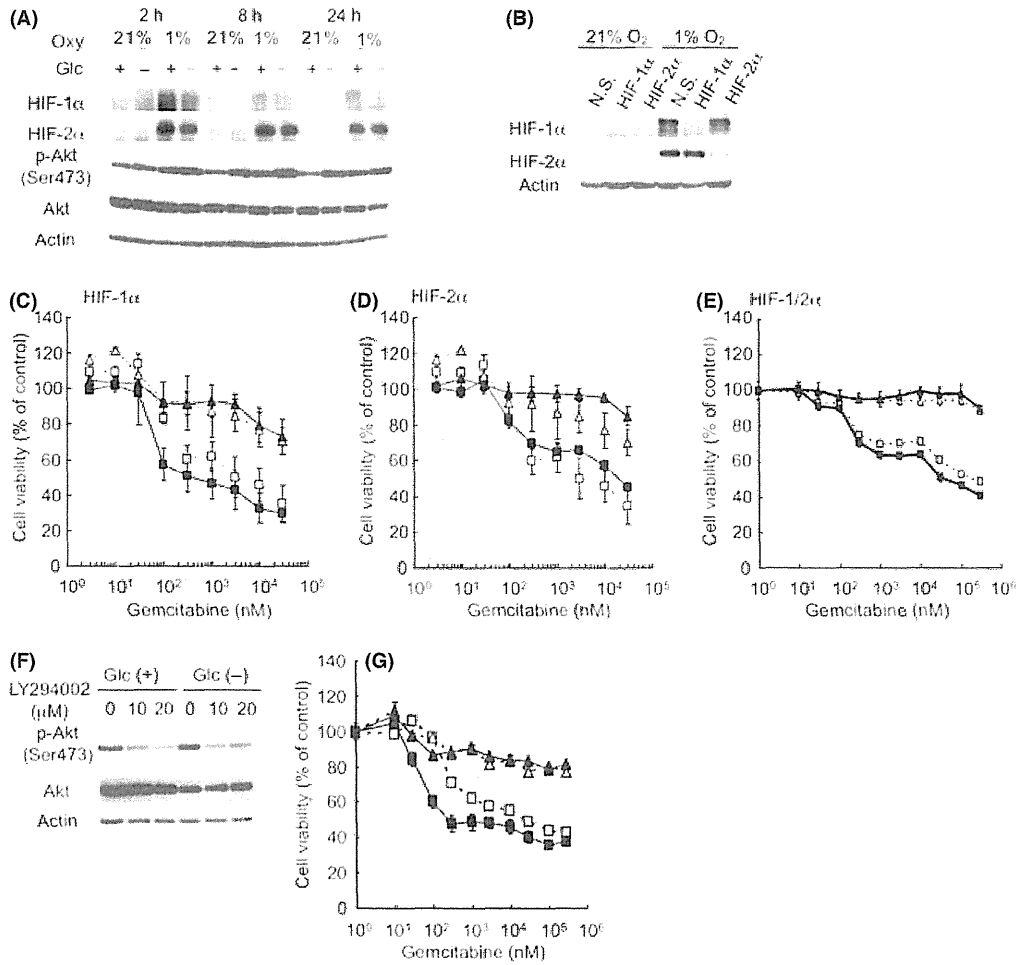

Fig. 4. Effects of inhibition of HIFs and PI3K/Akt signaling on the sensitivity of the cells to gemcitabine. (A) Western blot analysis for HIF1α and 2α accumulation and Akt phosphorylation under the indicated oxygen tension, normoxia (21%), or hypoxia (1%), and in the presence of a glucose concentration of 1 g/L (+) or 0 g/L (−). (B) Western blot analysis for HIF1α and 2α protein in cells treated with HIF-1α or HIF-2α siRNA. The cytotoxicity of gemcitabine on (C) HIF-1α, (D) HIF-2α or (E) HIF-1/2α knockdown cells or control cells under (■ or □) normoglycemic/normoxic condition or (▲ or △) normoglycemic/hypoxic condition. (F) Phosphorylation of Akt in the presence of 10 or 20 μM LY294002 under the indicated culture conditions. (G) Cytotoxicity of gemcitabine in the presence or absence of 20 μM LY294002 under (■ or □) normoglycemic/normoxic condition or (▲ or △) hypoglycemic/normoxic condition.

HIF signaling: HIF-1α, HIF-2α, or HIF-1/2α knockdown cells were examined for their sensitivity to gemcitabine in the presence of 1 μM UCN-01; however, even such combined inhibition was found to have no effect on the sensitivity of the cells to gemcitabine under the hypoxic condition (Fig. 5).

Effect of combined inhibition of Chk1 and PI3K signaling on the drug resistance induced by hypoglycemic/hypoxic condition. Combined inhibition of Chk1 and PI3K signaling was examined. As shown in Figure 6 1μM UCN-01 and 20 μM LY294002 strongly enhanced gemcitabine cytotoxicity under both normoglycemic/normoxic and hypoglycemic/hypoxic conditions, although the effect under the hypoglycemic/hypoxic condition was less pronounced (Fig. 6A). On the other hand, combined treatment with 1 μM Gö6976 and 20 μM LY294002 enhanced the sensitivity of the cells to gemcitabine only under the normoglycemic/normoxic condition (Fig. 6B). In order to confirm if the effect of UCN-01 was due to inhibition of Chk1 activation or inhibition of some other target, the effect of the RNAi on Chk1 activation was examined. Chk1 siRNA and 20 μM LY294002 enhanced the sensitivity of the cells to gemcitabine under the normoglycemic/normoxic condition; however, it had no any effect under the hypoglycemic/hypoxic condition.

Discussion

As clearly shown in the present work, hypoxia and hypoglycemia had a large impact on the cellular sensitivity to anticancer drugs in different cancer cell lines. In most cases, the mechanism underlying the drug resistance is regarded as decreased cellular drug uptake. Multidrug resistance is one of major cellular mechanisms of drug resistance to a broad spectrum of anticancer drugs, and this phenotype is associated with an increased drug efflux from the cells caused by overexpression of the ABC transporter. In the present work, hypoglycemic/hypoxic condition also induced multidrug resistance; however, our findings clearly indicated that there was no reduction of gemcitabine uptake and incorporation under the hypoglycemic/hypoxic condition. The S-phase population was similar under the normoglycemic/normoxic and hypoglycemic/hypoxic conditions, with accompanying S-phase prolongation. S-phase prolongation might be due to the depletion of *de novo* synthesis of nucleotides caused by

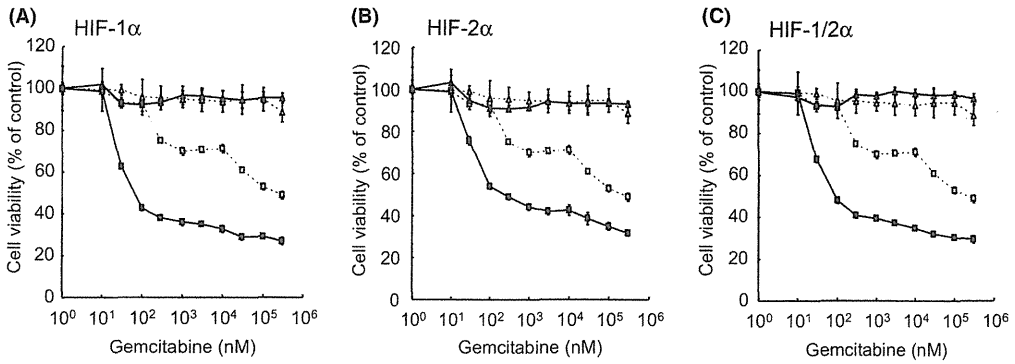

Fig. 5. Effect of combined inhibition of Chk1 and HIF signaling on the sensitivity of the cells to gemcitabine. Cells were treated with gemcitabine in the presence or absence of 1 μM UCN-01 plus RNAi for (A) HIF-1α, (B) HIF-2α or (C) HIF-1/2α under (■ or □) normoglycemic/normoxic condition or (▲ or △) normoglycemic/hypoxic condition.

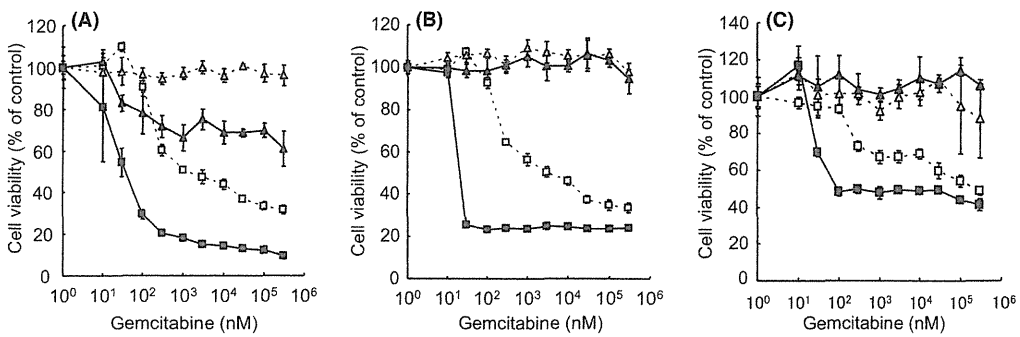

Fig. 6. Effect of combined inhibition of Chk1 and PI3K on the sensitivity of the cells to gemcitabine. Cells were treated with gemcitabine in the presence or absence of 1 μM (A) UCN-01, (B) 1 μM Gö6976 or (C) RNAi for Chk1, and 20 μM LY294002 under (■ or □) normoglycemic/normoxic condition or (▲ or △) hypoglycemic/hypoxic condition.

insufficiency of the pentose phosphate shunt supply. Nevertheless, it was not involved in DNA incorporation of gemcitabine under the hypoglycemic/hypoxic condition. Following its incorporation into DNA, gemcitabine blocks the extension of DNA and stall replication forks, leading to DNA damage. The DNA damage is recognized by sensor molecules that recruit and phosphorylate H2AX protein in the damaged DNA region.[44] Sensor molecules also phosphorylate checkpoint kinase causing its activation and arresting the cell cycle in the S phase.[45] The present study showed that phosphorylation of H2AX, Chk1 and Chk2 were induced by gemcitabine equally under the normoglycemic/normoxic and hypoglycemic/hypoxic conditions, leading to S-phase arrest. During checkpoint kinase activation and cell cycle arrest, phosphorylation of H2AX is known to be recruited by other DNA repair proteins, such as Mre11/Rad50/Nbs1, in the DNA damage region, resulting in activation of the DNA repair pathway.[46,47] Chronic hypoxia has been reported to suppress DNA repair protein activity.[48,49] The increased DNA incorporation of gemcitabine under the hypoglycemic/hypoxic condition may be caused by suppression of the DNA repair pathway.

Modulation of the cellular responses to DNA-damaging agents by checkpoint abrogators or inhibitors of cell survival signaling is an active area of research, since it has been believed that the interference of these signalings may enhance the therapeutic efficacy of anticancer drugs.[50] The S-phase checkpoint consists of a hierarchal regulatory cascade initiated by the activation of Chk1. In the present work, Chk1 inhibitors and Chk1 siRNA enhanced the cytotoxicity of gemcitabine under the normoglycemic/normoxic condition, consistent with other reports.[51–54] However, the abrogation of Chk1 activation did not affect the sensitivity of the cells to gemcitabine under the hypoglycemic/hypoxic condition. Tumor hypoxia has been well-studied, and previous reports have proposed that HIF-1α plays a critical role in determining cell survival and death,[40,41] while knockdown of HIF1α or HIF2α using siRNA did not affect the sensitivity of the cells to gemcitabine under the hypoxic condition in the present study. The PI3K/Akt pathway is well-known for its anti-apoptotic and cell survival activity under various conditions, including hypoxia and hypoglycemia,[55–57] but our results showed that the PI3K inhibitor LY294002 sensitized the cells to gemcitabine only under the normoglycemic/normoxic condition. We examined combined inhibition of Chk1 and of the cell survival pathways-sensitized cells to gemcitabine under the hypoglycemic/hypoxic condition. In the present work, the combination of UCN-01 and LY294002 partly abrogated the hypoglycemic/hypoxia-induced drug resistance, whereas the combination of Gö6976 or Chk1 siRNA with LY294002 had no such effect. These observations suggest that UCN-01 had a different target from Gö6976 in the mechanism of sensitizing the cells to gemcitabine under the hypoglycemic/hypoxic condition. UCN-01 has been reported to induce apoptosis in S-phase-arrested cells, not through Chk1 inhibition, although the precise mechanisms remain poorly understood.[58] We attempted to identify the kinase signaling responsible for the hypoglycemic/hypoxia-induced drug resistance in the targets of UCN-01; however, we did not obtain any clear results. PI3K and Akt are strongly expressed in some cancers, and have been found to be associated with a poor prognosis and increased tumor aggressiveness.[59,60] We previously reported that Akt

doi: 10.1111/j.1349-7006.2011.01880.x

expression was closely associated with cellular tolerance for nutrient deprivation.[61] The present work showed that Akt phosphorylation had a significant impact on the sensitivity of the PANC-1 cells to anticancer drugs.

In this study, we showed that hypoglycemic/hypoxic condition induced multidrug resistance. Combined kinase activations were involved in the hypoglycemic/hypoxia-induced drug resistance. Although the mechanism of cell death caused by gemcitabine is still unclear, the combined strategies described in the text might enhance the cytotoxicity of gemcitabine in clinical practice.

Acknowledgments

This work was supported by a Grant for the Third-Term Comprehensive 10-year Strategy for Cancer Control and 5-year Strategy for the Creation of Innovative Pharmaceuticals and Medical Devices from the Ministry of Health, Labour and Welfare, Japan.

Disclosure statement

No conflict of interest.

References

1 Jain RK. Molecular regulation of vessel maturation. *Nat Med* 2003; **9**: 685–93.
2 Thomlinson RH, Gray LH. The histological structure of some human lung cancers and the possible implications for radiotherapy. *Br J Cancer* 1955; **9**: 539–49.
3 Less JR, Skalak TC, Sevick EM, Jain RK. Microvascular architecture in a mammary carcinoma: branching patterns and vessel dimensions. *Cancer Res* 1991; **51**: 265–73.
4 Brown JM, Giaccia AJ. The unique physiology of solid tumors: opportunities (and problems) for cancer therapy. *Cancer Res* 1998; **58**: 1408–16.
5 Hockel M, Vaupel P. Tumor hypoxia: definitions and current clinical, biologic, and molecular aspects. *J Natl Cancer Inst* 2001; **93**: 266–76.
6 Harris AL. Hypoxia – a key regulatory factor in tumour growth. *Nat Rev Cancer* 2002; **2**: 38–47.
7 Bertout JA, Patel SA, Simon MC. The impact of O_2 availability on human cancer. *Nat Rev Cancer* 2008; **8**: 967–75.
8 Gatenby RA, Gillies RJ. Why do cancers have high aerobic glycolysis? *Nat Rev Cancer* 2004; **4**: 891–9.
9 Gillies RJ, Raghunand N, Karczmar GS, Bhujwalla ZM. MRI of the tumor microenvironment. *J Magn Reson Imaging* 2002; **16**: 430–50.
10 Semenza GL. HIF-1, O(2), and the 3 PHDs: how animal cells signal hypoxia to the nucleus. *Cell* 2001; **107**: 1–3.
11 Price BD, Calderwood SK. Gadd45 and Gadd153 messenger RNA levels are increased during hypoxia and after exposure of cells to agents which elevate the levels of the glucose-regulated proteins. *Cancer Res* 1992; **52**: 3814–7.
12 Wang GL, Semenza GL. Characterization of hypoxia-inducible factor 1 and regulation of DNA binding activity by hypoxia. *J Biol Chem* 1993; **268**: 21513–8.
13 Ryan HE, Lo J, Johnson RS. HIF-1 alpha is required for solid tumor formation and embryonic vascularization. *The EMBO J* 1998; **17**: 3005–15.
14 Maxwell PH, Dachs GU, Gleadle JM *et al.* Hypoxia-inducible factor-1 modulates gene expression in solid tumors and influences both angiogenesis and tumor growth. *Proc Natl Acad Sci U S A* 1997; **94**: 8104–9.
15 Carmeliet P, Dor Y, Herbert JM *et al.* Role of HIF-1alpha in hypoxia-mediated apoptosis, cell proliferation and tumour angiogenesis. *Nature* 1998; **394**: 485–90.
16 Warburg O. On the origin of cancer cells. *Science* 1956; **123**: 309–14.
17 Vander Heiden MG, Cantley LC, Thompson CB. Understanding the Warburg effect: the metabolic requirements of cell proliferation. *Science* 2009; **324**: 1029–33.
18 Chen Z, Lu W, Garcia-Prieto C, Huang P. The Warburg effect and its cancer therapeutic implications. *J Bioenerg Biomembr* 2007; **39**: 267–74.
19 Kondoh H. Cellular life span and the Warburg effect. *Exp Cell Res* 2008; **314**: 1923–8.
20 Hirayama A, Kami K, Sugimoto M *et al.* Quantitative metabolome profiling of colon and stomach cancer microenvironment by capillary electrophoresis time-of-flight mass spectrometry. *Cancer Res* 2009; **69**: 4918–25.
21 Savage P, Stebbing J, Bower M, Crook T. Why does cytotoxic chemotherapy cure only some cancers? *Nat Clin Pract Oncol* 2009; **6**: 43–52.
22 Minchinton AI, Tannock IF. Drug penetration in solid tumours. *Nat Rev Cancer* 2006; **6**: 583–92.
23 Tsuruo T, Naito M, Tomida A *et al.* Molecular targeting therapy of cancer: drug resistance, apoptosis and survival signal. *Cancer Sci* 2003; **94**: 15–21.
24 Sugimoto Y, Tsuruo T. DNA-mediated transfer and cloning of a human multidrug-resistant gene of adriamycin-resistant myelogenous leukemia K562. *Cancer Res* 1987; **47**: 2620–5.
25 Hamada H, Tsuruo T. Functional role for the 170- to 180-kDa glycoprotein specific to drug-resistant tumor cells as revealed by monoclonal antibodies. *Proc Natl Acad Sci U S A* 1986; **83**: 7785–9.
26 Ho WJ, Pham EA, Kim JW *et al.* Incorporation of multicellular spheroids into 3-D polymeric scaffolds provides an improved tumor model for screening anticancer drugs. *Cancer Sci* 2010; **101**: 2637–43.
27 Liao Q, Hu Y, Zhao YP, Zhou T, Zhang Q. Assessment of pancreatic carcinoma cell chemosensitivity using a three-dimensional culture system. *Chin Med J (Engl)* 2010; **123**: 1871–7.
28 Lu J, Kunimoto S, Yamazaki Y, Kaminishi M, Esumi H. Kigamicin D, a novel anticancer agent based on a new anti-austerity strategy targeting cancer cells' tolerance to nutrient starvation. *Cancer Sci* 2004; **95**: 547–52.
29 Awale S, Lu J, Kalauni SK *et al.* Identification of arctigenin as an antitumor agent having the ability to eliminate the tolerance of cancer cells to nutrient starvation. *Cancer Res* 2006; **66**: 1751–7.
30 Wong SJ, Myette MS, Wereley JP, Chitambar CR. Increased sensitivity of hydroxyurea-resistant leukemic cells to gemcitabine. *Clin Cancer Res* 1999; **5**: 439–43.
31 Imamura T, Kanai F, Kawakami T *et al.* Proteomic analysis of the TGF-beta signaling pathway in pancreatic carcinoma cells using stable RNA interference to silence Smad4 expression. *Biochem Biophys Res Commun* 2004; **318**: 289–96.
32 Sampath D, Rao VA, Plunkett W. Mechanisms of apoptosis induction by nucleoside analogs. *Oncogene* 2003; **22**: 9063–74.
33 Ewald B, Sampath D, Plunkett W. Nucleoside analogs: molecular mechanisms signaling cell death. *Oncogene* 2008; **27**: 6522–37.
34 Zhang YW, Hunter T, Abraham RT. Turning the replication checkpoint on and off. *Cell Cycle* 2006; **5**: 125–8.
35 Sampath D, Shi Z, Plunkett W. Inhibition of cyclin-dependent kinase 2 by the Chk1-Cdc25A pathway during the S-phase checkpoint activated by fludarabine: dysregulation by 7-hydroxystaurosporine. *Mol Pharmacol* 2002; **62**: 680–8.
36 Facchinetti MM, De Siervi A, Toskos D, Senderowicz AM. UCN-01-induced cell cycle arrest requires the transcriptional induction of p21(waf1/cip1) by activation of mitogen-activated protein/extracellular signal-regulated kinase kinase/extracellular signal-regulated kinase pathway. *Cancer Res* 2004; **64**: 3629–37.
37 Monks A, Harris ED, Vaigro-Wolff A, Hose CD, Connelly JW, Sausville EA. UCN-01 enhances the in vitro toxicity of clinical agents in human tumor cell lines. *Invest New Drugs* 2000; **18**: 95–107.
38 Ewald B, Sampath D, Plunkett W. H2AX phosphorylation marks gemcitabine-induced stalled replication forks and their collapse upon S-phase checkpoint abrogation. *Mol Cancer Ther* 2007; **6**: 1239–48.
39 Kohn EA, Yoo CJ, Eastman A. The protein kinase C inhibitor Go6976 is a potent inhibitor of DNA damage-induced S and G2 cell cycle checkpoints. *Cancer Res* 2003; **63**: 31–5.
40 Semenza GL. Targeting HIF-1 for cancer therapy. *Nat Rev Cancer* 2003; **3**: 721–32.
41 Koukourakis MI, Giatromanolaki A, Sivridis E *et al.* Hypoxia-inducible factor (HIF1A and HIF2A), angiogenesis, and chemoradiotherapy outcome of squamous cell head-and-neck cancer. *Int J Radiat Oncol Biol Phys* 2002; **53**: 1192–202.
42 Chen EY, Mazure NM, Cooper JA, Giaccia AJ. Hypoxia activates a platelet-derived growth factor receptor/phosphatidylinositol 3-kinase/Akt pathway that results in glycogen synthase kinase-3 inactivation. *Cancer Res* 2001; **61**: 2429–33.
43 Esumi H, Izuishi K, Kato K *et al.* Hypoxia and nitric oxide treatment confer tolerance to glucose starvation in a 5′-AMP-activated protein kinase-dependent manner. *J Biol Chem* 2002; **277**: 32791–8.
44 Bonner WM, Redon CE, Dickey JS *et al.* GammaH2AX and cancer. *Nat Rev Cancer* 2008; **8**: 957–67.
45 Tse AN, Carvajal R, Schwartz GK. Targeting checkpoint kinase 1 in cancer therapeutics. *Clin Cancer Res* 2007; **13**: 1955–60.
46 Ewald B, Sampath D, Plunkett W. ATM and the Mre11-Rad50-Nbs1 complex respond to nucleoside analogue-induced stalled replication forks and contribute to drug resistance. *Cancer Res* 2008; **68**: 7947–55.
47 Parsels LA, Morgan MA, Tanska DM *et al.* Gemcitabine sensitization by checkpoint kinase 1 inhibition correlates with inhibition of a Rad51 DNA damage response in pancreatic cancer cells. *Mol Cancer Ther* 2009; **8**: 45–54.

48 Chan N, Koritzinsky M, Zhao H *et al.* Chronic hypoxia decreases synthesis of homologous recombination proteins to offset chemoresistance and radioresistance. *Cancer Res* 2008; **68**: 605–14.
49 Bristow RG, Hill RP. Hypoxia and metabolism Hypoxia, DNA repair and genetic instability. *Nat Rev Cancer* 2008; **8**: 180–92.
50 Skladanowski A, Bozko P, Sabisz M, Larsen AK. Dual inhibition of PI3K/Akt signaling and the DNA damage checkpoint in p53-deficient cells with strong survival signaling: implications for cancer therapy. *Cell Cycle* 2007; **6**: 2268–75.
51 Morgan MA, Parsels LA, Parsels JD, Mesiwala AK, Maybaum J, Lawrence TS. Role of checkpoint kinase 1 in preventing premature mitosis in response to gemcitabine. *Cancer Res* 2005; **65**: 6835–42.
52 Morgan MA, Parsels LA, Parsels JD, Lawrence TS, Maybaum J. The relationship of premature mitosis to cytotoxicity in response to checkpoint abrogation and antimetabolite treatment. *Cell Cycle* 2006; **5**: 1983–8.
53 Matthews DJ, Yakes FM, Chen J *et al.* Pharmacological abrogation of S-phase checkpoint enhances the anti-tumor activity of gemcitabine in vivo. *Cell Cycle* 2007; **6**: 104–10.
54 Karnitz LM, Flatten KS, Wagner JM *et al.* Gemcitabine-induced activation of checkpoint signaling pathways that affect tumor cell survival. *Mol Pharmacol* 2005; **68**: 1636–44.
55 Pham NA, Tsao MS, Cao P, Hedley DW. Dissociation of gemcitabine sensitivity and protein kinase B signaling in pancreatic ductal adenocarcinoma models. *Pancreas* 2007; **35**: e16–26.
56 Klein JB, Barati MT, Wu R *et al.* Akt-mediated valosin-containing protein 97 phosphorylation regulates its association with ubiquitinated proteins. *J Biol Chem* 2005; **280**: 31870–81.
57 Yokoi K, Fidler IJ. Hypoxia increases resistance of human pancreatic cancer cells to apoptosis induced by gemcitabine. *Clin Cancer Res* 2004; **10**: 2299–306.
58 Shi Z, Azuma A, Sampath D, Li YX, Huang P, Plunkett W. S-Phase arrest by nucleoside analogues and abrogation of survival without cell cycle progression by 7-hydroxystaurosporine. *Cancer Res* 2001; **61**: 1065–72.
59 Cheng JQ, Ruggeri B, Klein WM *et al.* Amplification of AKT2 in human pancreatic cells and inhibition of AKT2 expression and tumorigenicity by antisense RNA. *Proc Natl Acad Sci U S A* 1996; **93**: 3636–41.
60 Ruggeri BA, Huang L, Wood M, Cheng JQ, Testa JR. Amplification and overexpression of the AKT2 oncogene in a subset of human pancreatic ductal adenocarcinomas. *Mol Carcinog* 1998; **21**: 81–6.
61 Izuishi K, Kato K, Ogura T, Kinoshita T, Esumi H. Remarkable tolerance of tumor cells to nutrient deprivation: possible new biochemical target for cancer therapy. *Cancer Res* 2000; **60**: 6201–7.

doi: 10.1111/j.1349-7006.2011.01880.x

JJCO Japanese Journal of Clinical Oncology

Jpn J Clin Oncol 2011;41(2)239–244
doi:10.1093/jjco/hyq216
Advance Access Publication 26 November 2010

Biased Discordance of *KRAS* Mutation Detection in Archived Colorectal Cancer Specimens Between the ARMS–Scorpion Method and Direct Sequencing

Hideaki Bando[1,2], Katsuya Tsuchihara[1], Takayuki Yoshino[2], Motohiro Kojima[3], Naomi Ogasawara[1], Hiraku Fukushima[2], Atsushi Ochiai[3], Atsushi Ohtsu[2] and Hiroyasu Esumi[1,*]

[1]Cancer Physiology Project, Research Center for Innovative Oncology, National Cancer Center Hospital East, [2]Division of Gastrointestinal Oncology, National Cancer Center Hospital East and [3]Pathology Division, Research Center for Innovative Oncology, National Cancer Center Hospital East, Kashiwa, Japan

*For reprints and all correspondence: Hiroyasu Esumi, National Cancer Center Hospital East, 6-5-1 Kashiwanoha, Kashiwa, Chiba 277-8577, Japan. E-mail: hesumi@east.ncc.go.jp

Received June 7, 2010; accepted October 23, 2010

Objective: The concordance of *KRAS* mutation detection between the amplification refractory mutation system–Scorpion assay and direct sequencing was evaluated with clinically available formalin-fixed, paraffin-embedded specimens of metastatic colorectal cancers.
Methods: Genomic DNA from 120 macrodissected specimens was examined by the amplification refractory mutation system–Scorpion assay and direct sequencing. DNA mixtures of wild-type and mutant *KRAS* genes were prepared from the peripheral blood and the SW620 human colon cancer cell line for the model experiments.
Results: *KRAS* mutation was identified in 50 samples (41.7%) by the amplification refractory mutation system–Scorpion assay and 42 samples (35.0%) by direct sequencing. Discordance between the two methods was observed for samples with smaller amounts of amplifiable DNA. The sensitivity of direct sequencing was impaired by the decrease in template DNA and polymerase chain reaction cycles in the experimental models.
Conclusions: Decreased sensitivity of direct sequencing caused by insufficient polymerase chain reaction amplification resulted in biased discordance between direct sequencing and amplification refractory mutation system–Scorpion. Polymerase chain reaction conditions satisfactory for amplifying tens of haploid copies of genomic DNA to the saturation level might be necessary to ensure the robustness of the direct sequencing-based method employed for formalin-fixed, paraffin-embedded specimen-derived DNA samples.

Key words: ARMS–Scorpion – colorectal cancer – direct sequencing – formalin-fixed paraffin-embedded specimen – KRAS

INTRODUCTION

Retrospective subset analyses and prospective randomized Phase III clinical trials strongly suggest that patients with metastatic colorectal cancer (mCRC) containing *KRAS* gene mutations do not benefit from treatment with anti-epidermal growth factor receptor antibodies (1–4). On the basis of this evidence, pre-use *KRAS* mutation testing has been strongly recommended. Various methods have been developed for detecting *KRAS* mutation. A mutation-specific real-time polymerase chain reaction (PCR)-based technique combining amplification refractory mutation system (ARMS) and a unique bi-functional fluorescent primer/probe molecule (Scorpion) is one of the recommended methods for clinical use according to its robustness and convenience (5–11). Mutant alleles are selectively amplified by ARMS, and these amplified PCR products are sensitively and specifically detected by the Scorpion system. A standardized commercial kit based on the ARMS–Scorpion (ARMS/S) system allows the detection of seven major mutations in codons 12 and 13 of the *KRAS* gene present at low allelic concentrations (1%)

in heterogeneous specimens, with detection limits of between 5 and 10 copies. The kit has been used in several Phase III trials and is approved for use in *in vitro* diagnosis in EU countries (3).

Although various methods including ARMS/S have been developed, direct sequencing (DS) of PCR-amplified *KRAS* gene fragments is still one of the most clinically accessible methods. However, the low sensitivity of DS for mutant detection has been argued. DS is regarded as being most suitable for the detection of mutant alleles at an allelic concentration of more than 10–30%. To reduce the rate of false-negative errors in the diagnosis, macroscopic isolation of tissues in which cancer cells occupy more than 70% of the area (macrodissection) is recommended for retrieving genomic DNA samples (7).

We routinely employ both ARMS/S and the conventional DS for *KRAS* testing. Our data obtained from 120 formalin-fixed paraffin-embedded (FFPE) specimens revealed discordance in the detection of *KRAS* mutations between the two methods. Interestingly, the discordance was specifically observed in the samples with lower amounts of amplifiable DNA. Since such biased discordance could not be simply explained by the lower sensitivity of DS, we attempted to clarify the underlying reasons.

PATIENTS AND METHODS

Tissue Samples and DNA Extraction Used for Practice Investigations

Genomic DNA was obtained from primary and mCRC tissues of patients who were scheduled to receive treatment with cetuximab. Tissue samples were collected by surgical resection or biopsy at the National Cancer Center Hospital East (NCCHE) and other hospitals. The collections and investigations were conducted with the approval of the Institutional Review Board. In NCCHE, all specimens were fixed in 10% formalin for 1 day and then embedded in paraffin. From the FFPE tissue blocks, three to five slices of 10 μm-thick unstained sections were cut. Tissue areas in which tumor cells occupied more than 70% were macroscopically dissected and then genomic DNA was isolated using the QIAamp DNA FFPE Tissue Kit (Qiagen).

Control DNA Used for the Model System

Control DNA harboring wild-type *KRAS* gene and mutant *KRAS* gene, in which the 35th G residue of *KRAS* cDNA is mutated to T (c.35G > T), were purified from the whole blood cells of a healthy volunteer and the human colon cancer cell line SW620 which is homozygous for *KRAS* mutation (ATCC: CCL-227), respectively, for the model experiments. Total DNA from these samples was extracted using the DNeasy Blood & Tissue Kit (Qiagen).

ARMS/S Assay

KRAS mutations were detected using the K-RAS Mutation Test Kit (DxS-Qiagen), in accordance with the manufacturer's instructions. Purified genomic DNA (8–900 ng per reaction) was applied for a set of seven known *KRAS* mutation-detecting reactions and a control reaction. Reactions were allowed to proceed on a LightCycler 480 real-time PCR instrument (LC480) (Roche Diagnostics) and analyzed using LightCycler Adapt software, v1.1 (Roche Diagnostics). The presence of mutant alleles was determined by the difference in the cycle threshold (ΔC_t) value between the control and each of the mutant reactions. C_t is a number of the PCR cycles necessary to detect a fluorescent signal above the background signal, as a measure of the target molecules present at the beginning of the reaction. LightCycler Adapt software compares the sample ΔC_t values with the cut-off values for a 1% concentration of mutant alleles to identify the presence/absence of the mutation. To ensure the sensitivity to detect mutants present at 1%, the manufacturer suggests the use of DNA samples with control C_t values of <28.9.

PCR Amplification and DS of the *KRAS* Gene

The *KRAS* exon-2 fragment was amplified according to the method described in a previous report, but with some modification (1,12). Briefly, each 50 μl PCR cocktail contained genomic DNA, 1.5 mM of magnesium chloride, 200 μM of deoxynucleotide triphosphates, 0.2 μM of PCR primers and 2.5 U of HotStarTaq® DNA polymerase (Qiagen). The PCR conditions were as follows: 1 cycle at 95°C for 15 min; 35, 37 or 40 cycles at 95°C for 30 s, 55°C for 30 s and 72°C for 1 min; 1 cycle at 72°C for 10 min. Primer sequences were GTGTGACATGTTCTAATATAGTCA and GAATGGTCC TGCACCAGTAA. The PCR products were purified by Microcon centrifugal Filter devices (Millpore), and the amplicon size and amount were confirmed by DNA agarose gel electrophoresis. The purified PCR products were directly sequenced with the same primers as those used for the PCR. The BigDye Terminator v3.1 Cycle Sequencing Kit and ABI PRISM 3100 (Applied Biosystems) were used in accordance with the manufacturer's instructions. Analyses of the DNA sequences were performed with the Sequence Scanner Software, ver. 1.0 (Applied Biosystems). The signal intensity of each sequence peak was determined based on both the raw and the analyzed data view of the software.

Statistical Analysis

Fisher's exact test, ANOVA and Tukey's HSD procedure were used to compare the test results. Analyses were conducted with the JMP® 8 package software (SAS Institute, Cary, NC, USA).

RESULTS

Biased Discordance of Mutation Detection Between ARMS/S Assay and DS

A total of 120 colorectal cancer specimens (103 primary and 17 metastatic tumor specimens) collected from 112 patients were analyzed. Tumor DNA was isolated from tumor cell-rich tissue areas obtained by macrodissection. *KRAS* mutation was identified in 50 samples (41.7%) by the ARMS/S assay and 42 samples (35.0%) by DS. The results were stratified according to the C_t value of the control assays of the ARMS/S system. Among the samples with a control C_t value of <28.9, both the ARMS/S assay and DS identified the mutation in 18 of 46 samples (39.1%), whereas among the samples with a control C_t value of >29.0, the mutation was detected in 32 of 74 samples (43.2%) by the ARMS/S assay and in 24 of 74 samples (32.4%) by DS. Thus, the concordance rate was significantly lower among the samples with higher levels of control C_t (Table 1).

Table 1. Correlation between the control C_t value and the frequency of detection of the *KRAS* mutation

Control C_t	Incidence of mutation		Concordance between the two methods (%)
	Direct sequencing	ARMS–Scorpion	
<28.9	18/46 (39.1%)	18/46 (39.1%)	100.0%
>29.0	24/74 (32.4%)*	32/74 (43.2%)	86.5%*
Total	42/120 (35.0%)	50/120 (41.6%)	91.7%

ARMS, amplification refractory mutation system.
*Significantly different from the values in the specimens containing template DNA equivalent to <28.9 of the control C_t at a level of $P = 0.0130$ (two-tailed Fischer's exact test).

Enhancement of Mutant Signal Detection of DS by Increase in the Template DNA Extracted from the FFPE Specimens

The above findings implied that the amount of the template DNA influenced the sensitivity of DS. Therefore, in a subsequent experiment, seven specimens that had been determined as harboring wild-type *KRAS* by DS using a small amount of the template DNA (median: 160.0 ng, range: 54.6–212.9 ng) were selected and retested by DS using an increased amount of the template (median: 408.1 ng, range: 118.5–895.8 ng). Three of the seven samples examined were then found to exhibit apparent traces of the mutation. The three samples had been identified as harboring the *KRAS* mutation by the initial ARMS/S assay (Table 2 and Fig. 1A).

Table 2. Conversion of the nucleotide sequences of the *KRAS* gene by increase in the amount of the template DNA

Sample	Experiment 1		Experiment 2		ARMS–Scorpion
	DNA amount (ng)	Interpretation	DNA amount (ng)	Interpretation	
A	114.5	GGT	895.8	GGT	12Ala
B	179.9	GGT	839.2	GGT	Wild-type
C	160.0	GGT	494.9	G(G/A)T	12Asp
D	126.8	GGT	408.1	G(G/T)T	12Val
E	54.6	GGT	118.5	G(G/T)T	12Val
F	177.5	GGT	329.1	GGT	Wild-type
G	212.9	GGT	385.4	GGT	Wild-type

Decrease in Minor Mutant Signal Detection by DS Caused by Small Amounts of the Template DNA

To confirm the above DNA amount-dependent decreased detection power of DS, the following model experiment was carried out. A DNA mixture containing 10% of colon cancer cell line-derived genomic DNA harboring the homologous c.35G > T mutation and 90% of wild-type DNA was prepared (10% mutation DNA). Since our preliminary result revealed that 3.0 ng of intact genomic DNA yielded a control C_t value of 29 in the ARMS/S system (data not shown), 3.0 ng of 10% mutation DNA was serially diluted and 0.75, 0.19 and 0.05 ng of the DNA mixtures were examined by both the ARMS/S assay and DS. The mutant signals detected by DS using 3.0 ng DNA were specifically diminished when 0.75 and 0.19 ng of DNA were used. Neither wild-type nor mutant signals were detected with 0.05 ng of DNA. In the ARMS/S system, although the control C_t value increased as the amount of DNA decreased, the ΔC_t (difference between the mutation assay C_t and control assay C_t) did not differ among the results obtained using 3.0, 0.75 and 0.19 ng of DNA (Table 3 and Fig. 1B). The control C_t value was over 35 with 0.05 ng of DNA, and no mutant signals were detected even with 40 cycles of amplification when this amount of DNA was used.

Enhancement of the Sensitivity of DS by Increasing the Number of PCR Cycles

We further evaluated whether an increased number of PCR cycles might improve the sensitivity of DS obtained using a small amount of template DNA. The above-mentioned serially diluted 10% mutation DNA was amplified using 35 cycles and also using an increased number of PCR cycles of 37 and 40, then applied to the sequencing. With an increase in the number of PCR cycles, mutant signals became evident even with 0.05 ng of the template DNA (Table 3).